2013

Oxidation of Gold Clusters by Thiols

Brian M. Barngrover
Stephen F Austin State University, barngrovbm@sfasu.edu

Christine M. Aikens

THE JOURNAL OF PHYSICAL CHEMISTRY A

Article

pubs.acs.org/JPCA

Oxidation of Gold Clusters by Thiols

Brian M. Barngrover and Christine M. Aikens*

Department of Chemistry, Kansas State University, Manhattan, Kansas 66506, United States

ABSTRACT: The formation of gold−thiolate nanoparticles via oxidation of gold clusters by thiols is examined in this work. Using the BP86 density functional with a triple ζ basis set, the adsorption of methylthiol onto various gold clusters Au_n^Z (n = 1−8, 12, 13, 20; Z = 0, −1, +1) and Au_{38}^{4+} is investigated. The rate-limiting step for the reaction of one thiol with the gold cluster is the dissociation of the thiol proton; the resulting hydrogen atom can move around the gold cluster relatively freely. The addition of a second thiol can lead to H_2 formation and the generation of a gold−thiolate staple motif.

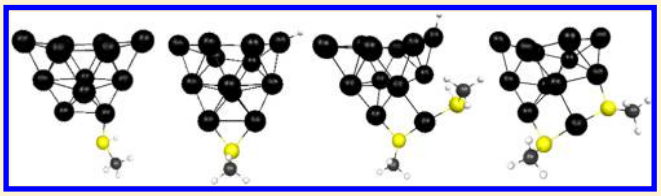

INTRODUCTION

Gold−thiolate nanoparticles and self-assembled monolayers (SAMs) are important for a variety of applications.[1−3] Recent structural studies using X-ray crystallography, scanning tunneling microscopy (STM), or density functional theory (DFT) on nanoparticles and SAMs have demonstrated that these systems have a core−shell-like arrangement in which gold−thiolate oligomers −SR−(Au−SR−)$_n$− (where the gold atom is formally considered to be in the +1 oxidation state) can cover a gold core or surface (which primarily contains Au(0)). For example, oligomeric motifs (often called "staples") are seen on a wide variety of nanoparticles such as $Au_{25}(SR)_{18}^{-/0}$,[4−7] $Au_{36}(SR)_{24}$,[8] $Au_{38}(SR)_{24}$,[9,10] and $Au_{102}(SR)_{44}$,[11] although recent work suggests that other binding motifs may be possible for sterically demanding thiolates.[12,13] These staples are also present on SAMs.[14−17]

The growth of gold−thiolate nanoparticles is often accomplished by the Brust−Schiffrin synthesis, in which a gold(III) salt reacts with thiol (HSR) and $NaBH_4$ and is consequently reduced to form $Au_n(SR)_m$ nanoparticles.[18] An alternative method of formation is through the use of solvated metal atom dispersion (SMAD), in which atoms from a metal vapor are trapped in frozen solvent such as tetrahydrofuran (THF) at 77 K, warmed to yield clusters and colloids, and subsequently reacted with thiol.[19] These two synthetic methods can yield different sizes of gold−thiolate nanoparticles.[20]

Because the properties of a gold nanoparticle depend on its size and morphology, understanding its growth mechanism is of interest because this can potentially lead to control over these aspects. Several experimental[21−23] and theoretical[24,25] studies have begun to examine the Brust−Schiffrin synthesis and determine whether thiols are able to play a role in reducing the Au(III) salt to a nanoparticle containing Au(0) and Au(I). However, little is known about the oxidative synthesis in which thiols oxidize bare gold clusters to yield $Au_n(SR)_m$ nanoparticles. Two experimental studies have shown that H_2 is released in this process.[26,27] A very recent theoretical study used ab initio molecular dynamics with DFT to examine the interaction of two thiols with an Au_4 cluster; they found that H_2 is produced in the reaction and a staple is formed on the gold cluster.[28] Methylthiolates adsorbed on bare Au_{38} clusters have also been observed by Jiang et al. to form staple motifs in dynamic simulations.[29] In this work, we examine reaction pathways for the interaction of small gold clusters Au_n (n = 1−8, 12, 13, 20, 38) with one and two thiols to determine the preferred adsorption sites for thiols, the rate-limiting step of hydrogen atom dissociation and transfer, and the thermodynamics of H_2 production and staple formation to provide a greater understanding of the oxidative growth mechanism of gold nanoparticles.

COMPUTATIONAL DETAILS

All calculations are performed with the Amsterdam density functional (ADF)[30] package, using density functional theory with the Becke Perdew (BP86)[31,32] functional and a frozen-core polarized triple-ζ (TZP) basis set. We include scalar relativistic effects by employing the zero-order regular approximation (ZORA).[33] We incorporate the THF solvent using the conductor-like screening model (COSMO), which represents the solvent by its dielectric constant.[34−36]

Initial structures for the small gold clusters Au_n (n = 1−8, 12, 13, 20, 38) are obtained from the literature;[37−42] both 2D and 3D structures for Au_{12} and Au_{13} are considered because these sizes are near the 2D−3D crossover point for gold.[41,42] Neutral, anionic, and cationic charge states for the gold clusters are examined, as discussed in the following section. Calculations described in this work employ the methyl group on the thiol or thiolate ligand. All intermediates and transition states are fully optimized; Hessian calculations have been performed to verify the existence of one imaginary frequency for the transition states.

Received: April 12, 2013
Revised: May 31, 2013
Published: June 5, 2013

   dx.doi.org/10.1021/jp403633a | J. Phys. Chem. A 2013, 117, 5377−5384

Table 1. Thiol Adsorption Energies for $Au_n^{(0,-,+)}$ (n = 1−8, 12, 13, 20) and Au_{38}^{4+}

neutral clusters	energy (eV)	anion clusters	energy (eV)	cation clusters	energy (eV)
Au_1	−0.68	Au_1	0.04	Au_1	−2.52
Au_2	−1.34	Au_2	NA	Au_2	−1.97
Au_3	−1.43	Au_3	NA	Au_3	−1.66
Au_4	−1.43	Au_4	−0.68	Au_4	−1.50
Au_5	−0.96	Au_5	−0.90	Au_5	−1.66
Au_6	−0.89	Au_6	−0.67	Au_6	−1.46
Au_7	−0.97	Au_7	−0.87	Au_7	−1.27
Au_8	−1.03	Au_8	−0.64	Au_8	−1.36
Au_{12} 2D	−0.90	Au_{12} 2D	−0.62	Au_{12} 2D	−1.21
Au_{12} 3D	−0.88	Au_{12} 3D	−0.55	Au_{12} 3D	−1.17
Au_{13} 2D	−0.98	Au_{13} 2D	−0.61	Au_{13} 2D	−1.40
Au_{13} 3D	−1.02	Au_{13} 3D	−0.63	Au_{13} 3D	−1.37
Au_{20}	−0.77	Au_{20}	−0.73	Au_{20}	−1.16
				Au_{38}^{4+}	−1.07

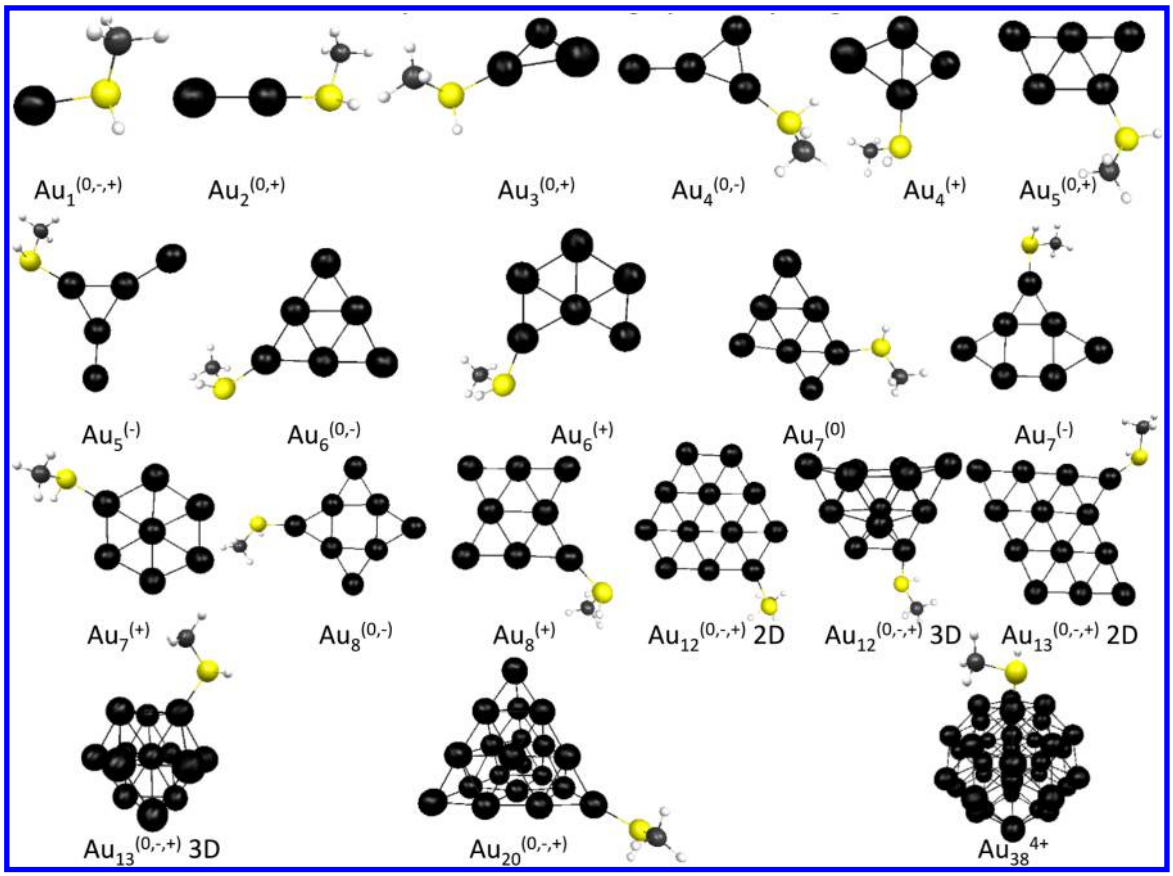

Figure 1. Lowest energy adsorption of methylthiol onto $Au_n^{(0,-,+)}$ (n = 1−8, 12, 13, 20) and Au_{38}^{4+}. Gold = black, sulfur = yellow, carbon = gray, and hydrogen = white.

RESULTS AND DISCUSSION

One Thiol Adsorption. Adsorption energies for one thiol on various gold clusters can be found in Table 1, and adsorption structures are shown in Figure 1. Binding of thiols to all unique gold coordinates were considered; only the lowest energy thiol adsorption sites are presented here. In almost all cases, thiol adsorption is exothermic. The first exception is the Au_1 anion, which is the only gold system examined here on which thiol adsorption is endothermic. Thiol adsorption on the neutral Au atom is exothermic with an adsorption energy (E_{ads}) of −0.68 eV, and adsorption on the Au_1^+ cation is the most favored with an adsorption energy of −2.52 eV. Thiol adsorption on all larger clusters is exothermic with the exception of Au_2^- and Au_3^- for which the thiol did not bind, which is in agreement with Varganov et al., who observed the same phenomenon with hydrogen on these clusters.[43] Because the thiol binds via lone pair donation to the gold cluster, it appears that the Au_n^- (n = 1−3) anions are too small to favorably accommodate this binding (possibly due to a high electron density). For Au_1 through Au_3, all of the charge states have the same lowest energy structure for a given cluster size. Au_4 has two different low-energy structures depending on charge: the neutral and anion share the same Y-shaped structure, whereas the cation has a diamond shape. As observed

dx.doi.org/10.1021/jp403633a | J. Phys. Chem. A 2013, 117, 5377−5384

Chart 1. Reaction Pathway of Thiol Adsorption on Au_3 and Subsequent Hydrogen Movement on the Gold Cluster[a]

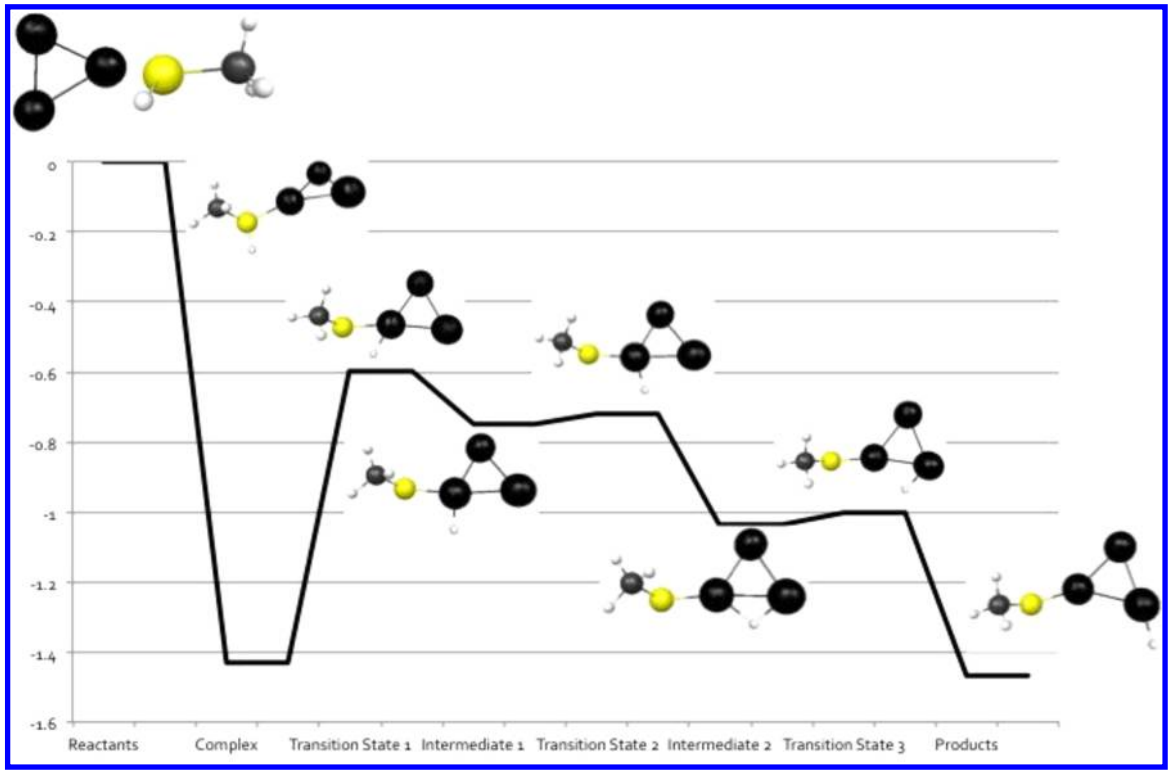

[a]Gold = black, sulfur = yellow, carbon = gray, and hydrogen = white.

Chart 2. Reaction Pathway of Thiol Adsorption on Au_{12} 3D and Subsequent Hydrogen Movement on the Gold Cluster[a]

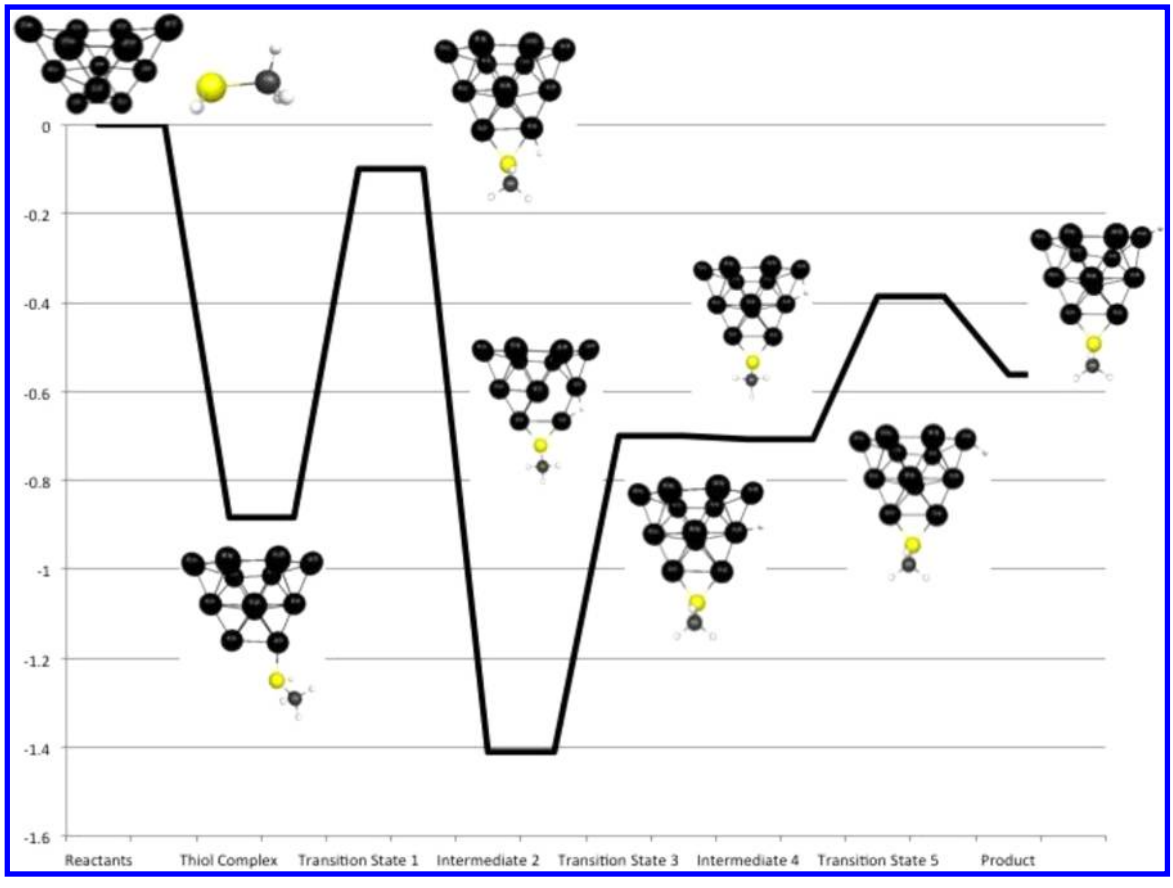

[a]Gold = black, sulfur = yellow, carbon = gray, and hydrogen = white.

dx.doi.org/10.1021/jp403633a | J. Phys. Chem. A 2013, 117, 5377−5384

for Au_1, the cation is the charge state for which thiol adsorption is the most favored, followed by the neutral state, and last the anionic charge state. Au_5 also has two different low-energy structures: Au_5^0 and Au_5^+ share the same W-shaped structure, whereas Au_5^- has a branched Y-shaped structure for its low-energy structure. The lowest energy structures for Au_1−Au_8 are indicated in Figure 1 with their corresponding charge states. The gold clusters with one thiol adsorbed have the same core structures as the bare systems. Even though various charge states have different lowest energy structures, the trend for favored adsorption continues with $|E_{ads}(\text{cation})| > |E_{ads}(\text{neutral})| > |E_{ads}(\text{anion})|$.

For Au_{12}, both 2D and 3D structures were considered with three different charge states because this cluster size is approximately where the 2D to 3D crossover occurs. At the BP86/TZP level of theory, the 2D structure is lower in energy than the 3D structure. The adsorption energy trend as a function of charge state continues even with the change in dimension. Au_{13} 2D and 3D structures have also been examined. For this system, we have investigated the cuboctahedral structure, which is not the lowest energy 3D structure but is of interest due to its high symmetry. Previous studies have examined binding of the thiolate ion to the cuboctahedral Au_{13} cluster.[44,45] It should be noted that the Au_{13} 2D structure is lower in energy than this cuboctahedral structure. For Au_{20}, the tetrahedral structure is the lowest energy structure.[38] Again, the adsorption energy of the cation is the greatest, followed by the neutral and then the anion. The last cluster we examined was octahedral Au_{38}^{4+}. The +4 charge state was examined because the neutral cuboctahedral cluster distorts due to a Jahn−Teller distortion.[46,47] This +4 charge leads to a cluster with an electronic magic number of 34 electrons. The octahedral cluster has two unique gold coordination sites: one is an edge atom joining two hexagonal faces and one square face and the other is the face site in the center of each hexagonal face. The edge site is the more favored thiol adsorption site compared with the face site, which is logical because it has a lower coordination number.

Reaction Pathway. Next, we investigated the reaction pathway from the adsorption of one thiol on Au_3 and Au_{12} 3D to the formation of $HAu_x(SCH_3)$ to determine which step is the rate-limiting step. The reaction pathways for Au_3 and Au_{12} are shown in Charts 1 and 2. The first transition state is calculated for the dissociation of the thiol proton onto the gold cluster. For Au_3, this transition state lies 0.83 eV above the adsorbed complex; for Au_{12} 3D, the barrier height is 0.78 eV. When the thiol proton dissociates it gains partial charge from the gold cluster and behaves more like a hydrogen atom. Once the hydrogen is on the gold surface, it is free to move around the gold surface with relative ease, as shown by the barrier heights for the subsequent steps; for Au_3, the next largest barrier height is 0.03 eV. This ease of movement has been observed by other groups.[43,48] Au_{12} has a stable second intermediate, with the stability possibly due to the hydrogen bridging the two gold atoms, making the subsequent barrier height rather high at 0.71 eV; however, this barrier height is still smaller than the previously mentioned one for the thiol proton dissociation.

In Charts 1 and 2, the first transition state lies significantly below the energy of the separated reactants; in consequence, if energy transfer to metal vibrational modes or to solvent is slow enough, then this reaction will proceed easily. Because the gold clusters are not bare under experimental conditions, we have considered the effects of solvent (in this case, THF) adsorption on the reaction energies. THF binds to the Au_3 and Au_{12} 3D clusters with E_{ads} of −0.69 and −0.28, respectively. The reaction for the replacement of THF by a thiol (leading to the first intermediates shown in Charts 1 and 2) yields reaction energies of −0.74 and −0.60, respectively; the energy released in these reactions is not quite enough to overcome the thiol dissociation barrier, so an effective activation energy barrier should be observed under experimental conditions.

Because the proton removal step is the rate-limiting step for Au_3 and Au_{12} 3D, a further investigation into this barrier height for all of the neutral gold−thiol clusters has been performed. Proton removal barrier heights are presented in Table 2. Thiol

Table 2. Barrier Heights for the Dissociation of the Thiol Proton on Au_n^0 (n = 1−8, 12, 13, 20) and Au_{38}^{4+}

cluster size	energy (eV)
Au_1	0.87
Au_2	1.26
Au_3	0.83
Au_4	1.18
Au_5	1.10
Au_6	1.61
Au_7	0.86
Au_8	1.38
Au_{12} 2D	1.06
Au_{12} 3D	0.78
Au_{13} 2D	1.28
Au_{20}	1.56
Au_{38}^{4+}	1.55

proton dissociation on Au_1 through Au_8 is found to have barrier heights of 0.87, 1.26, 0.83, 1.18, 1.10, 1.61, 0.86, and 1.38 eV, respectively. An overall odd−even effect is observed, which we believe is due to the unpaired electron in the odd size clusters, which more easily allows the cluster to provide an electron to the incoming hydrogen, thus lowering the barrier height. On closer examination, the barrier height on Au_7 is significantly lower than clusters of neighboring sizes; this is because Au_7 undergoes an isomer change (Figure 2). For the remaining

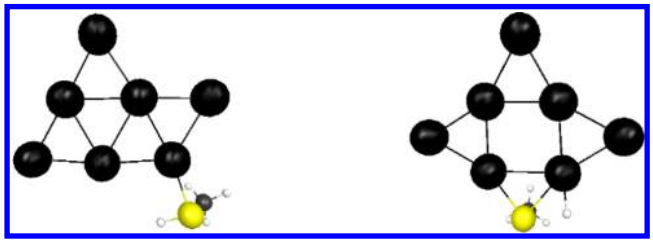

Figure 2. Isomer shift of Au_7 after the removal of the thiol proton and the formation of thiolate and hydrogen. Gold = black, sulfur = yellow, carbon = gray, and hydrogen = white.

larger clusters the pattern appears to hold true. Au_{12} 3D is also an interesting case to examine closer. The Au_{12} 3D structure forms a thiolate bridge between two gold atoms when the thiol proton is removed. This is only observed in this structure and Au_7.

Second Thiol Addition. The crux of this investigation is to develop an understanding of the formation of gold thiolate nanoclusters and hydrogen gas. To explore this, a second thiol is required. Structures resulting from the addition of a second

dx.doi.org/10.1021/jp403633a | J. Phys. Chem. A 2013, 117, 5377−5384

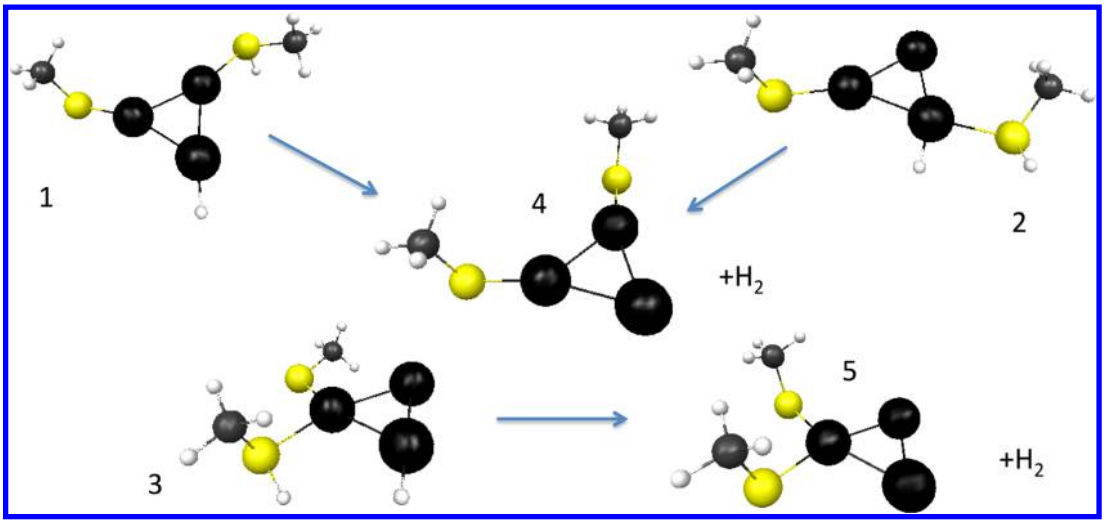

Figure 3. Second thiol adsorption to the vertices of Au_3. Structure 1: Second thiol binding to uncoordinated gold site. Structure 2: Second thiol coordinated to hydrogen site. Structure 3: Second thiol coordinated to thiolate site. Structure 4: Evolution of hydrogen gas and thiolate formation from structures 1 and 2. Structure 5: Evolution of hydrogen gas and thiolate formation from structure 3. Gold = black, sulfur = yellow, carbon = gray, and hydrogen = white.

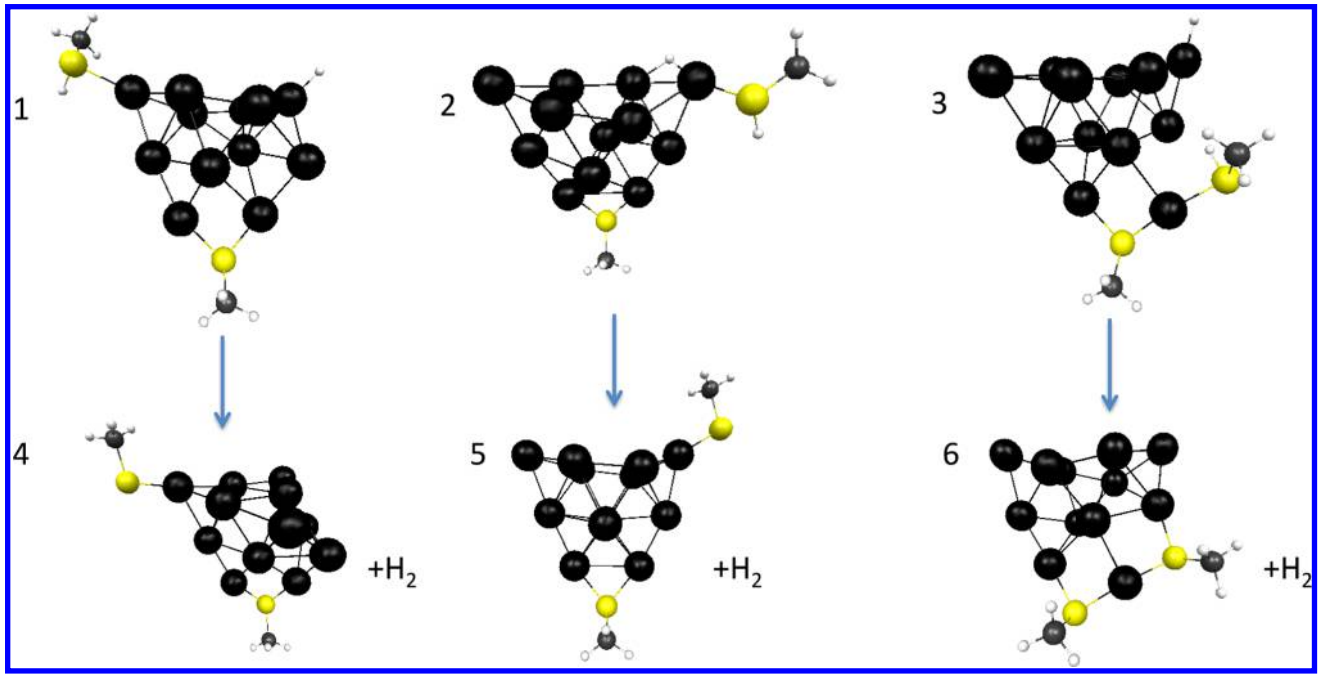

Figure 4. Second thiol adsorption to the vertices of Au_{12}. Structure 1: Second thiol binding to uncoordinated gold site. Structure 2: Second thiol coordinated to hydrogen site. Structure 3: Second thiol coordinated to thiolate site. Structure 4: Evolution of hydrogen gas and thiolate formation from structures 1. Structure 5: Evolution of hydrogen gas and thiolate formation from structure 2. Structure 6: Evolution of hydrogen gas and thiolate formation from structure 3. Gold = black, sulfur = yellow, carbon = gray, and hydrogen = white.

thiol to $HAu_3(SCH_3)$ and $HAu_{12}(SCH_3)$ 3D have been optimized. There are three sites for the incoming thiol to bind to on the Au_3 complex: where the thiolate is coordinated, where the hydrogen is coordinated, or on the uncoordinated gold (Figure 3). The favored adsorption site for the incoming thiol is the uncoordinated site (**1**) with an adsorption energy of −0.84 eV. The next favored adsorption site (**2**) is where the first hydrogen is coordinated with an adsorption energy of −0.41 eV. The least favored adsorption site (**3**) is where the first thiolate is coordinated with an adsorption energy of −0.14 eV. This trend makes sense because the incoming thiol would not have to compete with any other molecule or atom to bind to the uncoordinated site. The reaction energy for the production of hydrogen gas and a gold cluster with thiolates on different gold atoms (structure **4**) is −0.02 eV from structure **2** or 0.41 eV from structure **1**; the reaction energy is endothermic for the latter reaction because the initial structure has a high binding energy for the thiol. The least favored reaction is the production of H_2 from structure **3**, where the thiol and thiolate are coordinated to the same gold; this process has a reaction energy of 0.83 eV.

Compared to Au_3, Au_{12} 3D has many additional sites that the second thiol could adsorb to; in this work, we focus on the low-energy sites that are the other vertices. Unlike the Au_3 case, the

dx.doi.org/10.1021/jp403633a | J. Phys. Chem. A 2013, 117, 5377−5384

Chart 3. Reaction Pathway of Thiol Adsorption on $HAu_{12}SCH_3$ 3D and Subsequent Hydrogen Movement on the Gold Cluster[a]

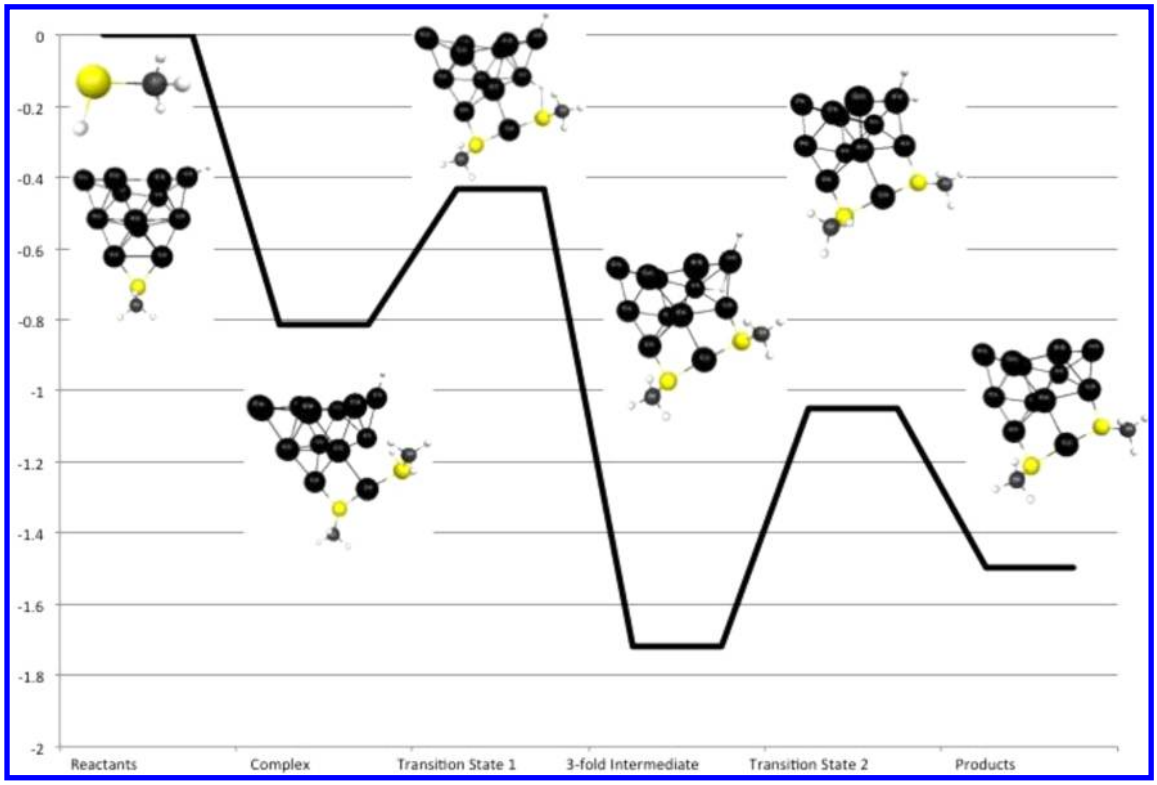

[a]Gold = black, sulfur = yellow, carbon = gray, and hydrogen = white.

thiol adsorbing to the vertex that was not coordinated to the thiolate or hydrogen (structure **1** in Figure 4) is not the most favored structure for Au_{12} 3D (E_{ads} = −1.02 eV). Instead, the lowest energy structure is structure **2**, in which the incoming thiol adsorbs to the gold atom where the hydrogen is coordinated (E_{ads} = −1.27 eV). The least favored adsorption site is structure **3**, where the thiolate is already adsorbed (E_{ads} = −0.81 eV). For both structures **1** and **2**, evolution of hydrogen gas is thermodynamically unfavorable; reaction energies to produce H_2 and structures **4** and **5** are 0.62 and 0.95 eV, respectively. In contrast, evolution of hydrogen gas from structure **3** is favorable with a reaction energy of −0.68 eV. The resulting structure **6** is also an interesting cluster because it is the first time formation of a staple motif is observed in this investigation. Structure **6** is lower in energy than isomers **4** and **5**, which underscores the importance of the staple motif in nanoparticle and SAM structure. Thus, although the most favorable adsorption geometries for thiols at low coverage involve low-coordinated gold atoms, these structures are not as likely to lead to the formation of staples and hydrogen gas. We expect that at higher coverages, such as those needed for full passivation of the nanoparticle surface, gold−thiolate staples will form.

A further investigation into the formation of structure **6** from structure **3** is examined (Chart 3). The removal of the thiol proton has a barrier height of 0.38 eV. An intermediate with a three-fold binding site for one of the hydrogens forms; this type of structure has not been seen in any of the previous pathways. The three-fold binding site is particularly stable with an energy of −1.72 eV. The transition state between the three-fold intermediate and the final evolution of hydrogen gas has a barrier height of 0.67 eV. During this potential energy surface investigation another interesting intermediate was found. This structure has two hydrogens that bridge the gold much like a staple motif (Figure 5). It is 0.02 eV more stable than the three-

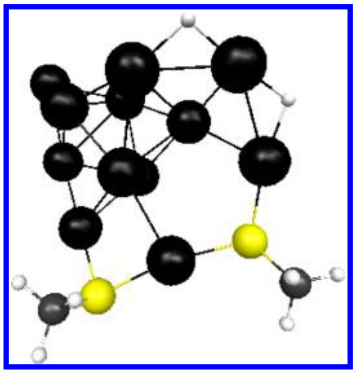

Figure 5. Bridging hydrogen motif structure. Gold = black, sulfur = yellow, carbon = gray, and hydrogen = white.

fold binding site with an energy of −1.74 eV relative to starting reactants. Although the barriers to form this intermediate are not known at this point, the staple-like motifs could be an interesting target for future experimental and theoretical investigations.

CONCLUSIONS

We investigated the adsorption of methylthiol onto various sizes of gold clusters (n = 1−8, 12, 13, 20, 38) with neutral, anionic, and cationic charge states (for Au_{38}, only the 4+ state was considered). We found that all adsorptions are predicted to be exothermic with the exceptions of Au_1^-, which is endothermic, and Au_2^- and Au_3^-, to which the thiol did not adsorb. We also determined that the rate-limiting step for the

dx.doi.org/10.1021/jp403633a | J. Phys. Chem. A 2013, 117, 5377−5384

formation of hydrogen gas and the gold thiolate staple motifs is the removal of the thiol proton. An odd−even effect on the formation of the thiolate and hydrogen is present; we conclude that the odd size clusters have a lower barrier height because they do not have to undergo drastic electronic rearrangement to accommodate the new additions to the cluster, whereas the even clusters would have to rearrange. The movement of the hydrogen atom on two specific gold clusters, Au_3 and Au_{12} 3D, was examined. The hydrogen moves easily around the clusters compared with the energy required to dissociate the hydrogen and form the thiolate on the cluster. One final step investigated was the formation of hydrogen gas. The adsorption of a second thiol to the vertices of Au_3 and Au_{12} 3D was considered. H_2 formation is thermodynamically favored relative to the energy of separated thiol and gold cluster but is not always exothermic once the second thiol has adsorbed to the gold cluster. Au_3 did not form a staple motif due to its small size, but a staple did form on Au_{12} 3D when the first and second thiol adsorbed to the same vertex. The most favorable adsorption geometries for thiols at low coverage involve nonadjacent gold atoms, but these structures are not likely to lead to the formation of staples and hydrogen gas. However at higher coverages, such as those present under most experimental conditions, gold−thiolate staples can form.

AUTHOR INFORMATION

Notes

The authors declare no competing financial interest.

ACKNOWLEDGMENTS

This material is based on work supported by the National Science Foundation under grant no. CHE-1213771.

REFERENCES

(1) Shiang, Y.-C.; Hsu, C.-L.; Huang, C.-C.; Chang, H.-T. Gold Nanoparticles Presenting Hybridized Self-Assembled Aptamers That Exhibit Enhanced Inhibition of Thrombin. *Angew. Chem., Int. Ed.* **2011**, *50*, 7660−7665.

(2) Loaiza, O. A.; Lamas-Ardisana, P. J.; Jubete, E.; Ochoteco, E.; Loinaz, I.; Cabañero, G.; García, I.; Penadés, S. Nanostructured Disposable Impedimetric Sensors as Tools for Specific Biomolecular Interactions: Sensitive Recognition of Concanavalin A. *Anal. Chem.* **2011**, *83*, 2987−2995.

(3) Wang, G.; Park, H.-Y.; Lipert, R. J.; Porter, M. D. Mixed Monolayers on Gold Nanoparticle Labels for Multiplexed Surface-Enhanced Raman Scattering Based Immunoassays. *Anal. Chem.* **2009**, *81*, 9643−9650.

(4) Heaven, M. W.; Dass, A.; White, P. S.; Holt, K. M.; Murray, R. W. Crystal Structure of the Gold Nanoparticle $[N(C_8H_{17})_4][Au_{25}(SCH_2CH_2Ph)_{18}]$. *J. Am. Chem. Soc.* **2008**, *130*, 3754−3755.

(5) Akola, J.; Walter, M.; Whetten, R. L.; Häkkinen, H.; Grönbeck, H. On the Structure of Thiolate-Protected Au_{25}. *J. Am. Chem. Soc.* **2008**, *130*, 3756−3757.

(6) Zhu, M.; Aikens, C. M.; Hollander, F. J.; Schatz, G. C.; Jin, R. Correlating the Crystal Structure of A Thiol-Protected Au_{25} Cluster and Optical Properties. *J. Am. Chem. Soc.* **2008**, *130*, 5883−5885.

(7) Zhu, M.; Eckenhoff, W. T.; Pintauer, T.; Jin, R. Conversion of Anionic $[Au_{25}(SCH_2CH_2Ph)_{18}]^-$ Cluster to Charge Neutral Cluster via Air Oxidation. *J. Phys. Chem. C* **2008**, *112*, 14221−14224.

(8) Zeng, C.; Qian, H.; Li, T.; Li, G.; Rosi, N. L.; Yoon, B.; Barnett, R. N.; Whetten, R. L.; Landman, U.; Jin, R. Total Structure and Electronic Properties of the Gold Nanocrystal $Au_{36}(SR)_{24}$. *Angew. Chem., Int. Ed.* **2012**, *124*, 13291−13295.

(9) Lopez-Acevedo, O.; Tsunoyama, H.; Tsukuda, T.; Häkkinen, H.; Aikens, C. M. Chirality and Electronic Structure of the Thiolate-Protected Au_{38} Nanocluster. *J. Am. Chem. Soc.* **2010**, *132*, 8210−8218.

(10) Qian, H.; Eckenhoff, W. T.; Zhu, Y.; Pintauer, T.; Jin, R. Total Structure Determination of Thiolate-Protected Au_{38} Nanoparticles. *J. Am. Chem. Soc.* **2010**, *132*, 8280−8281.

(11) Jadzinsky, P. D.; Calero, G.; Ackerson, C. J.; Bushnell, D. A.; Kornberg, R. D. Structure of a Thiol Monolayer-Protected Gold Nanoparticle at 1.1 Å Resolution. *Science* **2007**, *318*, 430−433.

(12) Krommenhoek, P. J.; Wang, J.; Hentz, N.; Johnston-Peck, A. C.; Kozek, K. A.; Kalyuzhny, G.; Tracy, J. B. Bulky Adamantanethiolate and Cyclohexanethiolate Ligands Favor Smaller Gold Nanoparticles with Altered Discrete Sizes. *ACS Nano* **2012**, *6*, 4903−4911.

(13) Nishigaki, J.-i.; Tsunoyama, R.; Tsunoyama, H.; Ichikuni, N.; Yamazoe, S.; Negishi, Y.; Ito, M.; Matsuo, T.; Tamao, K.; Tsukuda, T. A New Binding Motif of Sterically Demanding Thiolates on a Gold Cluster. *J. Am. Chem. Soc.* **2012**, *134*, 14295−14297.

(14) Maksymovych, P.; Sorescu, D. C.; Yates, J. T., Jr. Gold-Adatom-Mediated Bonding in Self-Assembled Short-Chain Alkanethiolate Species on the Au(111) Surface. *Phys. Rev. Lett.* **2006**, *97*, 146103.

(15) Cossaro, A.; Mazzarello, R.; Rousseau, R.; Casalis, L.; Verdini, A.; Kohlmeyer, A.; Floreano, L.; Scandolo, S.; Morgante, A.; Klein, M. L.; et al. X-ray Diffraction and Computation Yield the Structure of Alkanethiols on Gold(111). *Science* **2008**, *321*, 943−946.

(16) Grönbeck, H.; Häkkinen, H.; Whetten, R. L. Gold-Thiolate Complexes Form a Unique c(4 × 2) Structure on Au(111). *J. Phys. Chem. C* **2008**, *112*, 15490−15492.

(17) Jiang, D.-e.; Dai, S. Cis-trans Conversion of the CH_3S-Au-SCH_3 Complex on Au(111). *Phys. Chem. Chem. Phys.* **2009**, *97*, 146103.

(18) Brust, M.; Walker, M.; Bethell, D.; Schiffrin, D. J.; Whyman, R. Synthesis of Thiol-Derivatised Gold Nanoparticles in a Two-Phase Liquid-Liquid System. *J. Chem. Soc., Chem. Commun.* **1994**, 801.

(19) Stoeva, S.; Klabunde, K. J.; Sorensen, C. M.; Dragieva, I. Gram-Scale Synthesis of Monodisperse Gold Colloids by the Solvated Metal Atom Dispersion Method and Digestive Ripening and Their Organization into Two- and Three-Dimensional Structures. *J. Am. Chem. Soc.* **2002**, *124*, 2305−2311.

(20) Jose, D.; Matthiesen, J.; Parsons, C.; Sorensen, C. M.; Klabunde, K. J. Size Focusing of Nanoparticles by Thermodynamic Control through Ligand Interactions. Molecular Clusters Compared with Nanoparticles of Metals. *J. Phys. Chem. Lett.* **2012**, *3*, 885−890.

(21) Goulet, P. J. G.; Lennox, R. B. New Insights into Brust-Schiffrin Metal Nanoparticle Synthesis. *J. Am. Chem. Soc.* **2010**, *132*, 9582−9584.

(22) Li, Y.; Zaluzhna, O.; Xu, B.; Gao, Y.; Modest, J. M.; Tong, Y. J. Mechanistic Insights into the Brust-Schiffrin Two-Phase Synthesis of Organo-chalcogenate-Protected Metal Nanoparticles. *J. Am. Chem. Soc.* **2011**, *133*, 2092−2095.

(23) Li, Y.; Zaluzhna, O.; Tong, Y. J. Critical Role of Water and the Structure of Inverse Micelles in the Brust-Schiffrin Synthesis of Metal Nanoparticles. *Langmuir* **2011**, *27*, 7366−7370.

(24) Barngrover, B. M.; Aikens, C. M. Electron and Hydride Addition to Gold(I) Thiolate Oligomers: Implications for Gold-Thiolate Nanoparticle Growth Mechanisms. *J. Phys. Chem. Lett.* **2011**, *2*, 990−994.

(25) Barngrover, B. M.; Aikens, C. M. The Golden Pathway to Thiolate-Stabilized Nanoparticles: Following the Formation of Gold-(I) Thiolates from Gold(III) Chloride. *J. Am. Chem. Soc.* **2012**, *134*, 12590−12595.

(26) Petroski, J.; Chou, M.; Creutz, C. The Coordination Chemistry of Gold Surfaces: Formation and Far-Infrared Spectra of Alkanethiolate-Capped Gold Nanoparticles. *J. Organomet. Chem.* **2009**, *694*, 1138−1143.

(27) Matthiesen, J.; Jose, D.; Sorensen, C. M.; Klabunde, K. J. Loss of Hydrogen upon Exposure of Thiol to Gold Clusters at Low Temperature. *J. Am. Chem. Soc.* **2012**, *134*, 9376−9379.

(28) Rojas-Cervellera, V.; Giralt, E.; Rovira, C. Staple Motifs, Initial Steps in the Formation of Thiolate-Protected Gold Nanoparticles: How Do They Form? *Inorg. Chem.* **2012**, *51*, 11422−11429.

(29) Jiang, D.-e.; Tiago, M. L.; Luo, W.; Dai, S. The "Staple" Motif: A Key to Stability of Thiolate-Protected Gold Nanoclusters. *J. Am. Chem. Soc.* **2008**, *130*, 2777−2779.
(30) te Velde, G.; Bickelhaupt, F. M.; Baerends, E. J.; Fonseca Guerra, C.; van Gisbergen, S. J. A.; Snijders, J. G.; Ziegler, T. Chemistry with ADF. *J. Comput. Chem.* **2001**, *22*, 931−967.
(31) Becke, A. D. Density-Functional Exchange-Energy Approximation with Correct Asymptotic Behavior. *Phys. Rev. A* **1988**, *38*, 3098−3100.
(32) Perdew, J. P. Erratum: Density-Functional Approximation for the Correlation Energy of the Inhomogeneous Electron Gas. *Phys. Rev. B* **1986**, *34*, 7406−7406.
(33) van Lenthe, E.; Ehlers, A.; Baerends, E.-J. Geometry Optimizations in the Zero Order Regular Approximation for Relativistic Effects. *J. Chem. Phys.* **1999**, *110*, 8943−8953.
(34) Klamt, A. Conductor-like Screening Model for Real Solvents: A New Approach to the Quantitative Calculation of Solvation Phenomena. *J. Phys. Chem.* **1995**, *99*, 2224−2235.
(35) Klamt, A.; Jonas, V. Treatment of the Outlying Charge in Continuum Solvation Models. *J. Chem. Phys.* **1996**, *105*, 9972−9981.
(36) Klamt, A.; Schuurmann, G. COSMO: a New Approach to Dielectric Screening in Solvents with Explicit Expressions for the Screening Energy and Its Gradient. *J. Chem. Soc., Perkin Trans. 2* **1993**, 799−805.
(37) Häkkinen, H.; Yoon, B.; Landman, U.; Li, X.; Zhai, H.-J.; Wang, L.-S. On the Electronic and Atomic Structures of Small Au_N^- (N = 4−14) Clusters: A Photoelectron Spectroscopy and Density-Functional Study. *J. Phys. Chem. A* **2003**, *107*, 6168.
(38) Li, J.; Li, X.; Zhai, H.-J.; Wang, L.-S. Au20: A Tetrahedral Cluster. *Science* **2003**, *299*, 864.
(39) Walker, A. V. Structure and Energetics of Small Gold Nanoclusters and Their Positive Ions. *J. Chem. Phys.* **2005**, *122*, 094310.
(40) Xiao, L.; Tollberg, B.; Hu, X.; Wang, L. Structural Study of Gold Clusters. *J. Chem. Phys.* **2006**, *124*, 114309.
(41) Mantina, M.; Valero, R.; Truhlar, D. G. Validation Study of the Ability of Density Functionals to Predict the Planar-to-Three-Dimensional Structural Transition in Anionic Gold Clusters. *J. Chem. Phys.* **2009**, *131*, 064706.
(42) Li, X.-B.; Wang, H.-Y.; Yang, X.-D.; Zhu, Z.-H.; Tang, Y.-J. Size Dependence of the Structures and Energetic and Electronic Properties of Gold Clusters. *J. Chem. Phys.* **2007**, *126*, 084505.
(43) Varganov, S. A.; Olson, R. M.; Gordon, M. S.; Mills, G.; Metiu, H. A Study of the Reactions of Molecular Hydrogen with Small Gold Clusters. *J. Chem. Phys.* **2004**, *120*, 5169−5175.
(44) Larsson, J. A.; Nolan, M.; Greer, J. C. Interactions between Thiol Molecular Linkers and the Au_{13} Nanoparticle. *J. Phys. Chem. B* **2002**, *106*, 5931−5937.
(45) Genest, A.; Krüger, S.; Gordienko, A. B.; Rösch, N. Gold-Thiolate Clusters: A Relativistic Density Functional Study of the Model Species $Au_{13}(SR)_n$, R = H, CH_3, n = 4, 6, 8. *Z. Naturforsch.* **2004**, *59b*, 1585−1599.
(46) Michaelian, K.; Rendón, N.; Garzón, I. L. Structure and Energetics of Ni, Ag, and Au Nanoclusters. *Phys. Rev. B* **1999**, *60*, 2000−2010.
(47) Jiang, D.-e.; Walter, M. Au_{40}: A Large Tetrahedral Magic Cluster. *Phys. Rev. B* **2011**, *84*, 193402.
(48) Strømsnes, H.; Jusuf, S.; Schimmelpfennig, B.; Wahlgren, U.; Gropen, O. A Theoretical Study of the Chemisorption of Molecular Hydrogen on a Seven Atom Gold Cluster. *J. Mol. Struct.* **2001**, *567*−*568*, 137−143.